Inverse problem in optical diffusion tomography. I. Fourier–Laplace inversion formulas

Vadim A. Markel and John C. Schotland

Department of Electrical Engineering, Washington University, St. Louis, Missouri 63130-4899

Received April 21, 2000; revised manuscript received September 1, 2000; accepted December 13, 2000

We consider the inverse problem of reconstructing the absorption and diffusion coefficients of an inhomogeneous highly scattering medium probed by diffuse light. Inversion formulas based on the Fourier–Laplace transform are used to establish the existence and uniqueness of solutions to this problem in planar, cylindrical, and spherical geometries. © 2001 Optical Society of America

OCIS codes: 170.0170, 170.3010, 170.3660, 170.6960.

1. INTRODUCTION

There has been considerable recent interest in the use of diffuse light for biomedical imaging.[1–6] The basic physical problem consists of reconstructing the spatial distribution of the optical absorption and diffusion coefficients inside a highly scattering medium from intensity measurements with multiple sources and detectors. Although the applications discussed in the above references are biomedical, the problem of imaging in scattering media is of more general physical interest (see, for example, Ref. 7).

There are two fundamentally different approaches to imaging in highly scattering systems. The first approach is based on detection of only "ballistic" or "first transmitted" photons[8–17] with the use of optical gates that exclude multiply scattered light that is considered to be unsuitable for image formation. The second, more powerful approach is to directly use the multiply scattered light for image reconstruction,[18–28] which provides, in principle, the most complete information about the scattering medium. In this method, the forward scattering problem for diffuse light is inverted numerically[21,22] or analytically.[26] The equations describing scattering of the diffuse light from fluctuations in the absorption and diffusion coefficients $\delta\alpha$ and δD, respectively are in general nonlinear.[18,19,29] As a result, numerical reconstruction of these quantities is an extremely complicated problem. Although algorithms based on the nonlinear equations play an important role since they are in principle nonperturbative, a more practical method based on linearization of the forward problem is often employed. In this method, the integral equations of diffuse light propagation are expanded and linearized in $\delta\alpha$ and δD.[21,22,26] These equations can then be solved either by discretization and numerical solution of the resultant linear algebraic equations[21,22] or with the use of analytical inversion formulas.[26] Below, we will adopt the latter approach and use it to establish the existence and uniqueness of solutions to the inverse problem and to obtain inversion formulas in the planar, cylindrical, and spherical geometries of the measurement surfaces. These three geometrical settings are the most simple and experimentally important.

Both the absorption (α) and the diffusion (D) coefficients are functions of the three-dimensional position vector, while the scattering data is obtained from multiple measurements where both the sources and the detectors are located on fixed two-dimensional surfaces. Therefore the inverse problem of reconstruction of α and D from the four-dimensional scattering data is overdetermined. It is evident, however, from physical considerations that a solution to the inverse problem exists. Indeed, in an ideal experiment, the measured data are produced by some fluctuations of α and D, from which it follows that these quantities and the data must satisfy the diffusion equation. We will call such data "physically admissible". The uniqueness of the solution is a more complicated matter, and it has been established, for example, that in the case of cw tomography, α and D can not be simultaneously recovered in a unique way.[30] It is also well known from electrostatics that the scalar potential measured outside a sphere can be created by different distributions of charge inside the sphere. However, the inverse problem of diffusion tomography is essentially different from this electrostatic problem because the sources and detectors are located outside the medium to be imaged.

In this paper, we establish the existence and uniqueness of solutions to the inverse problem by bringing the equations to the Fourier–Laplace integral form, which is known to have a unique inverse. The proofs are constructive and lead directly to inversion formulas. An approach based on the Fourier–Laplace transform was first suggested in Ref. 26. The Fourier transformation was used in the planar geometry by various authors[31–34] to extract the transverse absorption coefficient $a(x,y)$ of a separable medium where α is of the form $\alpha(x,y,z) = a(x,y)\delta(z - z_0)$, and the depth z_0 of the thin slice where all inhomogeneities are localized is known *a priori*. Here we generalize the method of Ref. 26, which does not require any *a priori* information or that the medium is separable. In particular, we include reconstruction of the diffusion coefficient (possibly simultaneously with the absorption coefficient) and different geometrical settings of sources and detectors.

Throughout this paper we assume that the sources are stationary with a harmonically modulated intensity.

0740-3232/2001/061336-12$15.00

This approach can be easily generalized to pulsed sources by simple Fourier transformation from the frequency to the time domains. Obviously, the important parameter for pulsed sources is the pulse duration, as opposed to the modulation frequency for harmonic sources.

In the first paper in this series, we neglect the influence of boundaries on which sources and detectors are located. Boundary conditions will be the subject of the second paper in the series. In the third paper we will develop a practical method for numerical inversion of the Fourier–Laplace transform based on the singular-value decomposition of the Fourier–Laplace integral operator and will present results of numerical calculations.

The paper is organized as follows: We consider three different geometrical settings and for each setting discuss reconstruction of the absorption and diffusion coefficients separately and then simultaneously. After introducing the main equations in Section 2, we consider in detail the experimentally important case of the planar geometry (Section 3). We then consider the cylindrical (Section 4) and spherical (Section 5) geometries. In Section 6 we summarize and discuss the main results obtained.

2. BASIC EQUATIONS

We begin with the diffusion equation for the energy density $u(\mathbf{r}, t)$ of a diffusing wave produced by a time-dependent source $S(\mathbf{r}, t)$, which in its most general form can be written as

$$\frac{\partial u(\mathbf{r}, t)}{\partial t} = \nabla \cdot [D(\mathbf{r})\nabla u(\mathbf{r}, t)] - \alpha(\mathbf{r})u(\mathbf{r}, t) + S(\mathbf{r}, t), \tag{1}$$

where $D(\mathbf{r})$ and $\alpha(\mathbf{r})$ are the position-dependent diffusion and absorption coefficients. We decompose the diffusion and absorption coefficients as $D(\mathbf{r}) = D_0 + \delta D(\mathbf{r})$, $\alpha(\mathbf{r}) = \alpha_0 + \delta\alpha(\mathbf{r})$, where D_0 and α_0 are the average (background) values of the respective coefficients. We assume that the intensity sources are harmonically time-modulated according to $S(\mathbf{r}, t) = S(\mathbf{r})[1 + A\exp(-i\omega t)]$, where $A < 1$ is a constant. Then Eq. (1) assumes the following form:

$$(\nabla^2 - k^2)u(\mathbf{r}) = \frac{1}{D_0}[\delta\alpha(\mathbf{r}) - \nabla \cdot \delta D(\mathbf{r})\nabla]u(\mathbf{r}) - \frac{1}{D_0}S(\mathbf{r}), \tag{2}$$

where

$$\gamma(A) = \begin{cases} A & \text{if } \omega > 0 \\ 1 + A & \text{if } \omega = 0' \end{cases} \tag{3}$$

and the "diffuse" wave number k is given by

$$k^2 = \frac{\alpha_0 - i\omega}{D_0}, \tag{4}$$

and $u(\mathbf{r})$ is the Fourier component of $u(\mathbf{r}, t)$ with frequency ω. Since the energy density in the absence of sources is identically zero, the solution to Eq. (2) can be written as

$$u(\mathbf{r}) = \gamma(A)\int G_0(\mathbf{r}, \mathbf{r}')S(\mathbf{r}')\mathrm{d}^3r' + \int G_0(\mathbf{r}, \mathbf{r}') \times [\nabla_{\mathbf{r}'} \cdot \delta D(\mathbf{r}')\nabla_{\mathbf{r}'} - \delta\alpha(\mathbf{r}')]u(\mathbf{r}')\mathrm{d}^3r', \tag{5}$$

where $G_0(\mathbf{r}, \mathbf{r}')$ is the Green's function that satisfies the diffusion equation with $\delta\alpha = \delta D = 0$ and a point source:

$$(\nabla_{\mathbf{r}}^2 - k^2)G_0(\mathbf{r}, \mathbf{r}') = -\frac{1}{D_0}\delta(\mathbf{r} - \mathbf{r}'). \tag{6}$$

In general, $G_0(\mathbf{r}, \mathbf{r}')$ must also satisfy boundary conditions on surfaces where the sources and detectors are located. The boundary conditions will be considered in the second paper in this series. Here we do not consider the effects of boundaries and assume that G_0 is the Green's function in an infinite medium:

$$G_0(\mathbf{r}, \mathbf{r}') = \frac{\exp(-k|\mathbf{r} - \mathbf{r}'|)}{4\pi D_0|\mathbf{r} - \mathbf{r}'|}. \tag{7}$$

Note that expression (7) differs in the exponential factor $\exp(-k|\mathbf{r} - \mathbf{r}'|)$ [rather than $\exp(ik|\mathbf{r} - \mathbf{r}'|)$] from the usual retarded Green's function for the scalar-wave equation. Thus the propagation of diffusing waves in an absorbing medium differs from the propagation of scalar waves. Without modulation of the source, the wave number k is purely real for diffusing waves, which leads to exponential decay of G_0. For nonzero modulation frequency, k becomes complex but with a positive real part.

Since diffusion tomography employs multiple pointlike source–detector pairs, we assume that the source is located at the point $\mathbf{r}_1$ and the detector is located at the point $\mathbf{r}_2$: $S(\mathbf{r}) = S_0\delta(\mathbf{r} - \mathbf{r}_1)$. Then it readily follows from Eq. (5) that the diffuse light intensity at the point of observation $\mathbf{r}_2$ is given by $u(\mathbf{r}_2) = S_0\gamma(A)G(\mathbf{r}_1, \mathbf{r}_2)$, where A is the modulation amplitude and G is the Green's function that satisfies the integral equation

$$G(\mathbf{r}_1, \mathbf{r}_2) = G_0(\mathbf{r}_1, \mathbf{r}_2) + \int G_0(\mathbf{r}_1, \mathbf{r}) \times [\nabla_{\mathbf{r}} \cdot \delta D(\mathbf{r})\nabla D(\mathbf{r})\nabla_{\mathbf{r}} - \delta\alpha(\mathbf{r})]G(\mathbf{r}, \mathbf{r}_2)\mathrm{d}^3r. \tag{8}$$

To lowest order in perturbation theory in δD and $\delta\alpha$, the Green's function G is given by

$$G(\mathbf{r}_1, \mathbf{r}_2) = G_0(\mathbf{r}_1, \mathbf{r}_2) - \int G_0(\mathbf{r}_1, \mathbf{r})G_0(\mathbf{r}, \mathbf{r}_2)\delta\alpha(\mathbf{r})\mathrm{d}^3r - \int \nabla_{\mathbf{r}}G_0(\mathbf{r}_1, \mathbf{r}) \cdot \nabla_{\mathbf{r}}G_0(\mathbf{r}, \mathbf{r}_2)\delta D(\mathbf{r})\mathrm{d}^3r. \tag{9}$$

From the functional form of Eq. (9), we can conclude that $\delta\alpha$ and δD are coupled by an integral transformation to a data function that can be defined as

$$\phi(\mathbf{r}_1, \mathbf{r}_2) = G_0(\mathbf{r}_1, \mathbf{r}_2) - G(\mathbf{r}_1, \mathbf{r}_2). \tag{10}$$

This function can be obtained from multiple measurements with different source-detector pairs. The unperturbed Green's function is usually known analytically and can be verified by analogous measurements in a homogeneous (reference) medium. Therefore the main integral equation that we intend to invert in this paper is[35]

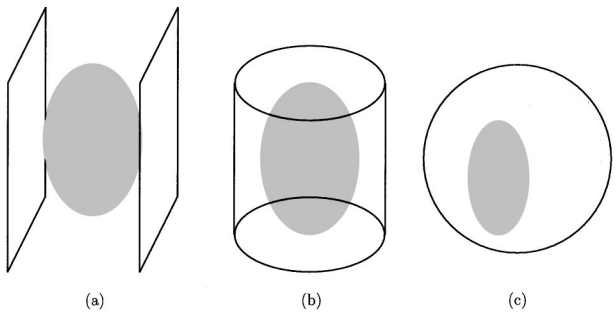

Fig. 1. Different geometrical arrangements of source-detector pairs. The gray areas indicate the objects to be imaged. In the case of (a) planar geometry, the sources and detectors can be placed either on the same plane or on different planes. For the cylindrical geometry (b), the sources and detectors are placed on the boundary of the cylinder, which is assumed to be infinitely long (much longer than the characteristic size of the sample). For the spherical geometry (c) the sources and detectors are placed on the surface of the sphere.

$$\phi(\mathbf{r}_1,\mathbf{r}_2) = \int G_0(\mathbf{r}_1,\mathbf{r})G_0(\mathbf{r},\mathbf{r}_2)\,\delta\alpha(\mathbf{r})\mathrm{d}^3r + \int \nabla_{\mathbf{r}}G_0(\mathbf{r}_1,\mathbf{r})\cdot\nabla_{\mathbf{r}}G_0(\mathbf{r},\mathbf{r}_2)\,\delta D(\mathbf{r})\mathrm{d}^3r. \tag{11}$$

We now recall some useful expansions of the Green's function $G_0(\mathbf{r}_1,\mathbf{r}_2)$ that will be in subsequent sections. The three-dimensional Fourier integral representation of $G_0(\mathbf{r}_1,\mathbf{r}_2)$ is given by

$$G_0(\mathbf{r}_1,\mathbf{r}_2) = \frac{1}{(2\pi)^3 D_0}\int \frac{\exp[i\mathbf{q}\cdot(\mathbf{r}_1-\mathbf{r}_2)]}{q^2+k^2}\mathrm{d}^3q. \tag{12}$$

This expansion is useful in the planar geometry illustrated in Fig. 1(a).

In the case of the cylindrical geometry [Fig. 1(b)] we require an expansion in terms of cylinder functions:

$$G_0(\rho_1,\varphi_1,z_1;\,\rho_2,\varphi_2,z_2) = \frac{1}{(2\pi)^2 D_0}\sum_{m=-\infty}^{\infty}\exp[im(\varphi_1-\varphi_2)] \times\int_{-\infty}^{\infty}\exp[iq(z_1-z_2)]K_m[(q^2+k^2)^{1/2}\rho_>] \times I_m[(q^2+k^2)^{1/2}\rho_<]\mathrm{d}q, \tag{13}$$

where we have used the cylindrical coordinate system $\mathbf{r} = (\rho,\varphi,z)$; $\rho_<$ and $\rho_>$ are the lesser and the greater of ρ_1 and ρ_2; and I_m, K_m are the modified Bessel and Hankel functions of the first kind.

Finally, in the spherical geometry [Fig. 1(c)] we use the expansion of G_0 in terms of the spherical functions

$$G_0(\mathbf{r}_1,\mathbf{r}_2) = \frac{k}{2\pi^2 D_0}\sum_{l=0}^{\infty}(2l+1)i_l(kr_<)k_l(kr_>)P_l(\hat{\mathbf{r}}_1\cdot\hat{\mathbf{r}}_2). \tag{14}$$

Here i_l and k_l are the modified spherical Bessel and Hankel functions, respectively; $P_l(x)$ are the Legendre polynomials; $r_<, r_>$ are the lesser and the greater of r_1, r_2; and $\hat{\mathbf{r}}_1, \hat{\mathbf{r}}_2$ are unit vectors pointing in the direction of $\mathbf{r}_1, \mathbf{r}_2$.

3. PLANAR GEOMETRY

We start with the planar geometry illustrated in Fig. 1(a). We consider the reconstruction of $\delta\alpha$ and δD separately and then show how they can be reconstructed simultaneously by using two different modulation frequencies.

A. Reconstruction of the Absorption Coefficient

Let us assume that $\delta D = 0$ and $\delta\alpha \neq 0$. We choose a cylindrical coordinate system $\mathbf{r} = (\boldsymbol{\rho}, z)$, where $\rho = |\boldsymbol{\rho}|$. The data function is measured on the surfaces $z = 0$ or $z = L$, depending on where the sources and detectors are located. We denote the z coordinate of the plane of sources by z_s and of the plane of detectors by z_d. Then, using the Fourier representation (12), we can write

$$\phi_\alpha(\boldsymbol{\rho}_1,z_s;\boldsymbol{\rho}_2,z_d) = \frac{1}{(2\pi)^6 {D_0}^2}\int \mathrm{d}^2\rho\mathrm{d}z\,\delta\alpha(\boldsymbol{\rho},z) \times\int \mathrm{d}^3p_1\mathrm{d}^3p_2\frac{\exp\{i[\mathbf{p}_{1\|}\cdot(\boldsymbol{\rho}_1-\boldsymbol{\rho}) + \mathbf{p}_{2\|}\cdot(\boldsymbol{\rho}-\boldsymbol{\rho}_2) + p_{1z}(z_d-z) + p_{2z}(z-z_s)]\}}{[(p_{1\|})^2+(p_{1z})^2+k^2][(p_{2\|})^2+(p_{2z})^2+k^2]}, \tag{15}$$

where $\|$ denotes the components of three-dimensional vectors $\mathbf{p}_{1,2}$ parallel to the planes of the sources and detectors. The subscript α in ϕ_α is used to emphasize that this is the scattering data produced by a nonzero $\delta\alpha$. We assume that $\delta\alpha(\boldsymbol{\rho},z)$ vanishes for $z<0$, $z>L$, and $\rho\to\infty$. Consequently, the data function also vanishes when $\rho_1\to\infty$ or $\rho_2\to\infty$, and we can define a Fourier transform of the data function according to

$$\phi_\alpha(\mathbf{q}_1,\mathbf{q}_2) = \int \mathrm{d}^2\rho_1\mathrm{d}^2\rho_2\,\phi_\alpha(\boldsymbol{\rho}_1,z_s;\boldsymbol{\rho}_2,z_d) \times\exp[i(\mathbf{q}_1\cdot\boldsymbol{\rho}_1+\mathbf{q}_2\cdot\boldsymbol{\rho}_2)], \tag{16}$$

where $\mathbf{q}_{1,2}$ are two-dimensional vectors parallel to the planes of the sources and detectors. We apply the transformation (16) to the integral equation (15), which results in

$$\phi_\alpha(\mathbf{q}_1,\mathbf{q}_2) = \int \mathrm{d}^2\rho\mathrm{d}z\,\delta\alpha(\mathbf{p},z)\frac{\exp[i(\mathbf{q}_1+\mathbf{q}_2)\cdot\boldsymbol{\rho} - Q(q_1)|z-z_s| - Q(q_2)|z-z_d|]}{(2D_0)^2 Q(q_1)Q(q_2)}, \tag{17}$$

where

$$Q(q) \equiv (\mathbf{q}^2 + k^2)^{1/2} \tag{18}$$

and we have used the result

$$\int_{-\infty}^{\infty} \frac{\exp(izt)\mathrm{d}t}{t^2 + q^2 + k^2} = \frac{\pi \exp[-Q(q)|z|]}{Q(q)}. \tag{19}$$

Now we restrict our attention to the case in which both the sources and the detectors are placed on the same plane. Without loss of generality, we can assume that $z_s = z_d = 0$ and $z > 0$. Results for the case in which sources and detectors are placed on different planes are discussed in Subsection 3.D. Assuming that the object to be imaged is in the right half-space $z > 0$, we obtain the following from Eq. (17):

$$\phi_\alpha(\mathbf{q}_1, \mathbf{q}_2) = \int \mathrm{d}^2\rho \mathrm{d}z\, \delta\alpha(\boldsymbol{\rho}, z) \times \frac{\exp[i(\mathbf{q}_1 + \mathbf{q}_2)\cdot\boldsymbol{\rho} - (Q(q_1) + Q(q_2))z]}{(2D_0)^2 Q(q_1)Q(q_2)}. \tag{20}$$

$$\mathbf{q}_{1,2} = \frac{\boldsymbol{\zeta}}{2} \pm \frac{\mathbf{e}_z \times \boldsymbol{\zeta}}{\zeta}\left[\left(\frac{\eta}{2}\right)^2 - \left(\frac{\zeta}{2}\right)^2 - k^2\right]^{1/2}. \tag{25}$$

Given solution (25), we can rewrite Eq. (17) as

$$\psi_\alpha(\boldsymbol{\zeta}, \eta) = \int \mathrm{d}^2\rho \mathrm{d}z\, \delta\alpha(\boldsymbol{\rho}, z)\exp(i\boldsymbol{\zeta}\cdot\boldsymbol{\rho} + \eta z), \tag{26}$$

with

$$\psi_\alpha(\boldsymbol{\zeta}, \eta) = (D_0\eta)^2 \phi_\alpha[\mathbf{q}_1(\boldsymbol{\zeta}, \eta), \mathbf{q}_2(\boldsymbol{\zeta}, \eta)]. \tag{27}$$

Equation (26) can now be formally inverted for $\delta\alpha$ as

$$\delta\alpha(\boldsymbol{\rho}, z) = \frac{1}{i(2\pi)^3}\int \mathrm{d}^2\zeta \int \mathrm{d}\eta \psi_\alpha(\boldsymbol{\zeta}, \eta)\exp(\eta z - i\boldsymbol{\zeta}\cdot\boldsymbol{\rho}), \tag{28}$$

where the integral over $\mathrm{d}\eta$ is taken along an infinite line parallel to the imaginary axis in the complex η plane.

To illustrate the use of the inversion formula (28), we consider the reconstruction of $\delta\alpha$ for a point absorber with $\delta\alpha(\mathbf{r}) = \alpha_0\delta(\boldsymbol{\rho} - \boldsymbol{\rho}_0)\delta(z - z_0)$. The data function is given by

$$\phi_\alpha(\boldsymbol{\rho}_1, 0; \boldsymbol{\rho}_2, 0) = \frac{\alpha_0}{(4\pi D_0)^2}\frac{\exp(-k\{[(\boldsymbol{\rho}_1 - \boldsymbol{\rho}_0)^2 + z_0^2]^{1/2} + [(\boldsymbol{\rho}_2 - \boldsymbol{\rho}_0)^2 + z_0^2]^{1/2}\})}{\{[(\boldsymbol{\rho}_1 - \boldsymbol{\rho}_0)^2 + z_0^2][(\boldsymbol{\rho}_2 - \boldsymbol{\rho}_0)^2 + z_0^2]\}^{1/2}}. \tag{29}$$

The above equation resembles the Fourier–Laplace transform of $\delta\alpha(\boldsymbol{\rho}, z)$, except that the prefactors in front of $\boldsymbol{\rho}$ and z do not formally coincide with the arguments of the data function $\phi_\alpha(\mathbf{q}_1, \mathbf{q}_2)$. To overcome this obstacle, we introduce an invertible transformation that maps the four-dimensional manifold $(\boldsymbol{\rho}_1, \boldsymbol{\rho}_2)$ onto a four-dimensional manifold $(\boldsymbol{\zeta}, \eta_1, \eta_2)$ according to

$$\boldsymbol{\zeta} = \mathbf{q}_1 + \mathbf{q}_2, \tag{21}$$

$$\eta_1 = 2Q(q_1), \tag{22}$$

$$\eta_2 = 2Q(q_2). \tag{23}$$

The Jacobian of this transformation can be easily found:

$$J = \frac{\partial(\boldsymbol{\zeta}, \eta_1, \eta_2)}{\partial(\mathbf{q}_1, \mathbf{q}_2)} = \frac{4(\mathbf{q}_2 \times \mathbf{q}_1)\cdot\hat{\mathbf{e}}_z}{Q(q_1)Q(q_2)}, \tag{24}$$

where $\hat{\mathbf{e}}_z$ is a unit vector in the z direction. As follows from Eq. (24), J vanishes only for collinear vectors $\mathbf{q}_1$ and $\mathbf{q}_2$. The submanifold of collinear $\mathbf{q}_1$ and $\mathbf{q}_2$ of the original four-dimensional manifold $(\mathbf{q}_1, \mathbf{q}_2)$ is of measure zero and can be neglected for our purposes.

The integral transformation (17) maps a function of a three-dimensional argument $\delta\alpha(\boldsymbol{\rho}, z)$ onto a function of a four-dimensional argument $\phi_\alpha(\mathbf{q}_1, \mathbf{q}_2)$, and the inverse problem is therefore overdetermined. We will show that it is sufficient to restrict the domain of the data function to a three-dimensional manifold defined by $q_1 = q_2 = q$ (in terms of the new variables, $\eta_1 = \eta_2 = \eta$). In this case, the solution to Eqs. (21)–(23) is given by

The Fourier transform of Eq. (29) can be easily obtained according to Eq. (16):

$$\phi_\alpha(\mathbf{q}_1, \mathbf{q}_2) = \frac{\alpha_0}{(2D_0)^2}\frac{\exp[i(\mathbf{q}_1 + \mathbf{q}_2)\cdot\boldsymbol{\rho}_0 - (Q(q_1) + Q(q_2))z_0]}{Q(q_1)Q(q_2)}. \tag{30}$$

Using the definitions (27) and Eqs. (21)–(23), and taking into account that $\eta_1 = \eta_2 = \eta$, we find that

$$\psi_\alpha(\boldsymbol{\zeta}, \eta) = \alpha_0 \exp(i\boldsymbol{\zeta}\cdot\boldsymbol{\rho}_0 - \eta z_0). \tag{31}$$

The inverse Fourier–Laplace transformation of this function according to Eq. (28) obviously results in the original distribution $\delta\alpha = \alpha_0\delta(\boldsymbol{\rho} - \boldsymbol{\rho}_0)\delta(z - z_0)$. Thus the inversion formula (28) was verified for a point absorber. From the linearity of integral equation (11), it can also be concluded that the inversion formula holds for arbitrary $\delta\alpha$.

It should be noted that for the Laplace part of the transformation in Eq. (28), integration can be carried out along the imaginary axis, $\eta = i\sigma$, where σ is real. This can be easily verified for a point absorber, but it also follows from the general fact that the Laplace transform (26) converges for $\eta = 0$ simply because $\delta\alpha$ vanishes for $z > L$. Therefore the inversion formula (28) can be written in a more specific form:

$$\delta\alpha(\boldsymbol{\rho}, z) = \frac{1}{(2\pi)^3}\int \mathrm{d}^2\zeta \int_{-\infty}^{\infty} \mathrm{d}\sigma \psi_\alpha(\boldsymbol{\zeta}, i\sigma) \times \exp[i(\sigma z - \boldsymbol{\zeta}\cdot\boldsymbol{\rho})]. \tag{32}$$

The inversion formula obtained in this subsection establishes the uniqueness of a solution to the inverse problem, provided that the data are physically admissible. In addition, the inversion formula (28) implicitly defines an inversion kernel for the integral equation (11). Indeed, we can define

$$K_\alpha(\boldsymbol{\rho}, z; \boldsymbol{\rho}_1, \boldsymbol{\rho}_2) = \frac{-D_0^2}{(2\pi)^3}\int_{-\infty}^{\infty} \mathrm{d}\sigma\sigma^2 \exp(i\sigma z) \times \int \mathrm{d}^2\zeta \exp\left\{ i\boldsymbol{\zeta}\cdot\left(\frac{\boldsymbol{\rho}_1+\boldsymbol{\rho}_2}{2}-\boldsymbol{\rho}\right) - \frac{\hat{\mathbf{e}}\times\boldsymbol{\zeta}}{\zeta}\cdot(\boldsymbol{\rho}_1-\boldsymbol{\rho}_2) \times [(\sigma/2)^2 + (\zeta/2)^2 + k^2]^{1/2}\right\}. \quad (33)$$

such that

$$\int \mathrm{d}^2\rho_1 \mathrm{d}^2\rho_2 K_\alpha(\boldsymbol{\rho}, z; \boldsymbol{\rho}_1, \boldsymbol{\rho}_2)\phi_\alpha(\boldsymbol{\rho}_1, \boldsymbol{\rho}_2) = \delta\alpha(\boldsymbol{\rho}, z), \quad (34)$$

or, equivalently,

$$\int \mathrm{d}^2\rho_1 \mathrm{d}^2\rho_2 K_\alpha(\boldsymbol{\rho}, z; \boldsymbol{\rho}_1, \boldsymbol{\rho}_2) G_0(\boldsymbol{\rho}_1, 0; \boldsymbol{\rho}', z') \times G_0(\boldsymbol{\rho}_2, 0; \boldsymbol{\rho}', z') = \delta(\boldsymbol{\rho}-\boldsymbol{\rho}')\delta(z-z'). \quad (35)$$

The inversion formula derived above requires an analytic continuation of the data function $\phi_\alpha(\mathbf{q}_1, \mathbf{q}_2)$ to complex values of $\mathbf{q}_1$ and $\mathbf{q}_2$. In the case of a point absorber, the analytic continuation is trivial, because an explicit formula for $\phi_\alpha(\mathbf{q}_1, \mathbf{q}_2)$ is available. In general, analytic continuation can pose a mathematical problem. However, a number of effective numerical methods for inversion of the Laplace transform that avoid analytic continuation have been developed and tested in application to such areas of physics as photon correlation spectroscopy,[36–38] chemical kinetics,[39] and nuclear physics.[40] In general, the robustness of the Laplace transform inversion can be greatly increased by utilizing some *a priori* information about the function being reconstructed.

B. Reconstruction of the Diffusion Coefficient

Now we assume in Eq. (11) that $\delta\alpha = 0$ and $\delta D \neq 0$. To facilitate the derivation of an inversion formula similar to the one in Subsection 3.B we retain the gradient operators in the integrand until the final step of the derivation. Using the Fourier representation (12), we can write Eq. (11) as

$$\phi_D(\boldsymbol{\rho}_1, \boldsymbol{\rho}_2) = \frac{1}{(2\pi)^6 D_0^2}\int \mathrm{d}^3 r\, \delta D(\boldsymbol{\rho}, z) \times \left[\nabla_{\mathbf{r}} \int \mathrm{d}^3 p_1 \frac{\exp[i\mathbf{p}_1\cdot(\boldsymbol{\rho}_1 + z_d\hat{\mathbf{e}}_z - \mathbf{r})]}{p_1^2 + k^2}\right] \cdot \left[\nabla_{\mathbf{r}} \int \mathrm{d}^3 p_2 \frac{\exp[i\mathbf{p}_2\cdot(\mathbf{r} - \boldsymbol{\rho}_2 - z_s\hat{\mathbf{e}}_s)]}{p_2^2 + k^2}\right], \quad (36)$$

where we have used the subscript D to emphasize that ϕ_D is the scattering data produced by a nonzero δD. After Fourier transformation of Eq. (36) according to Eq. (16), we obtain

$$\phi_D(\mathbf{q}_1, \mathbf{q}_2) = \frac{1}{(2D_0)^2 Q(q_1)Q(q_2)}\int \mathrm{d}^2\rho \mathrm{d}z\, \delta D(\boldsymbol{\rho}, z) \times [\nabla_{\mathbf{r}} \exp(i\mathbf{q}_1\cdot\boldsymbol{\rho} - Q(q_1)|z - z_s|)] \cdot [\nabla_{\mathbf{r}} \exp(i\mathbf{q}_2\cdot\boldsymbol{\rho} - Q(q_2)|z - z_d)]. \quad (37)$$

As before, we restrict consideration to the case in which both the sources and the detectors are located on the same plane ($z_s = z_d = 0$). The result is

$$\phi_D(\mathbf{q}_1, \mathbf{q}_2) = \frac{Q(q_1)Q(q_2) - \mathbf{q}_1\cdot\mathbf{q}_2}{(2D_0)^2 Q(q_1)Q(q_2)}\int \mathrm{d}^2\rho \mathrm{d}z\, \delta D(\boldsymbol{\rho}, z) \times \exp\{i(\mathbf{q}_1 + \mathbf{q}_2)\cdot\boldsymbol{\rho} - [Q(q_1) + Q(q_2)]z\}. \quad (38)$$

The above equation differs from Eq. (20) only by a multiplicative factor that is a function of $\mathbf{q}_1$ and $\mathbf{q}_2$. Using the definitions of $\boldsymbol{\zeta}$ and η introduced in the previous subsection, we can write, similar to Eqs. (26) and (27),

$$\psi_D(\boldsymbol{\zeta}, \eta) = \int \mathrm{d}^2\rho \mathrm{d}z\, \delta D(\boldsymbol{\rho}, z)\exp(i\boldsymbol{\zeta}\cdot\boldsymbol{\rho} + \eta z) \quad (39)$$

with

$$\psi_D(\boldsymbol{\zeta}, \eta) = \frac{(D_0\eta)^2}{\eta^2 - \zeta^2 - 2k^2}\phi_D[\mathbf{q}_1(\boldsymbol{\zeta}, \eta), \mathbf{q}_2(\boldsymbol{\zeta}, \eta)]. \quad (40)$$

We can solve Eq. (39) for δD by using Eq. (32). However, ψ is now given by Eq. (40) rather than by Eq. (27).

In a manner similar to the case considered in the Subsection 3.A, we can verify the inversion formulas (39) and (40) for a pointlike scatter with $\delta D(\boldsymbol{\rho}, z) = D_0\delta(\boldsymbol{\rho} - \boldsymbol{\rho}_0)\delta(z - z_0)$. The inversion kernel can be written as

$$K_D(\boldsymbol{\rho}, z; \boldsymbol{\rho}_1, \boldsymbol{\rho}_2) = \frac{2D_0^2}{(2\pi)^3}\int_{-\infty}^{\infty} \mathrm{d}\sigma\sigma^2 \exp(i\sigma z)\int \frac{\mathrm{d}^2\zeta}{\sigma^2 + \zeta^2 + 2k^2} \times \exp\left\{ i\boldsymbol{\zeta}\cdot\left(\frac{\boldsymbol{\rho}_1+\boldsymbol{\rho}_2}{2}-\boldsymbol{\rho}\right) - \frac{\hat{\mathbf{e}}_z\times\boldsymbol{\zeta}}{\zeta}\cdot(\boldsymbol{\rho}_1-\boldsymbol{\rho}_2) \times [(\sigma/2)^2 + (\zeta/2)^2 + k^2]^{1/2}\right\}. \quad (41)$$

C. Simultaneous Reconstruction of the Absorption and Diffusion Coefficients

In the general case, when $\delta\alpha \neq 0$ and $\delta D \neq 0$, we can combine the above derivations and write the Fourier-transformed data function as

$$\phi_{\mathrm{tot}}(\mathbf{q}_1,\mathbf{q}_2) = \frac{1}{(2D_0)^2 Q(q_1)Q(q_2)}\int \mathrm{d}^3 r\,\delta\alpha(\boldsymbol{\rho},z) \times \exp[i(\mathbf{q}_1+\mathbf{q}_2)\cdot\boldsymbol{\rho} - (Q(q_1)+Q(q_2))z] + \frac{Q(q_1)Q(q_2)-\mathbf{q}_1\cdot\mathbf{q}_2}{(2D_0)^2 Q(q_1)Q(q_2)}\int \mathrm{d}^3 r\,\delta D(\boldsymbol{\rho},z) \times \exp[i(\mathbf{q}_1+\mathbf{q}_2)\cdot\boldsymbol{\rho} - (Q(q_1)+Q(q_2))z]. \quad (42)$$

As above, we use the transformation [Eqs. (21)–(23)], and restrict consideration to the subspace $\eta_1 = \eta_2 = \eta$. Then Eq. (42) can be rewritten as

$$\phi_{\mathrm{tot}}(\boldsymbol{\zeta},\eta,k) = \int \mathrm{d}^2\rho\mathrm{d}z[c_\alpha(\boldsymbol{\zeta},\eta)\delta\alpha(\boldsymbol{\rho},z) + c_D(\boldsymbol{\zeta},\eta,k)\delta D(\boldsymbol{\rho},z)]\exp(i\boldsymbol{\zeta}\cdot\boldsymbol{\rho} - \eta z), \quad (43)$$

where we have indicated the explicit dependence on the wave number k. In particular, the quantities $\delta\alpha$ and δD under the integrals in the right-hand side of Eq. (43) do not depend explicitly on k. The dependence of c_α and c_D on their arguments is given by

$$c_\alpha(\boldsymbol{\zeta},\eta) = 1/(D_0\eta)^2, \quad (44)$$

$$c_D(\boldsymbol{\zeta},\eta,k) = (\eta^2/2 - \zeta^2/2 - k^2)/(D_0\eta)^2. \quad (45)$$

Thus, the coefficient c_D depends *explicitly* on k and therefore on the modulation frequency ω.

If we consider Eq. (43) for fixed values of $\mathbf{q}_1$ and $\mathbf{q}_2$ (with $\boldsymbol{\zeta}$ and η being the functions of the latter), there exists also an *implicit* dependence of the coefficients and integrands on k, since Eqs. (21)–(23) contain k as a parameter. However, it is possible to view the variables $\boldsymbol{\zeta}$, η, and k as mathematically independent. Indeed, suppose that we fix the variables $\boldsymbol{\zeta}$ and η and change k. In view of Eq. (25), this simply corresponds to using different values of $\mathbf{q}_1,\mathbf{q}_2$.

The left-hand side in Eq. (43) is the experimentally measurable data function. The right-hand side is given by a sum of two terms originating from nonzero values of $\delta\alpha$ and δD, namely, $c_\alpha\psi_\alpha$ and $c_D\psi_D$. The functions ψ_α and ψ_D can be used to calculate $\delta\alpha$ and δD by the inverse Fourier–Laplace transformation as described above, but they are not measurable separately. However, if we perform measurements at two different frequencies, ω_1 and ω_2 (with corresponding wave numbers k_1 and k_2), we obtain the system of equations

$$\phi_{\mathrm{tot}}(\boldsymbol{\zeta},\eta,k_1) = c_\alpha(\boldsymbol{\zeta},\eta)\psi_\alpha(\boldsymbol{\zeta},\eta) + c_D(\boldsymbol{\zeta},\eta,k_1)\psi_D(\boldsymbol{\zeta},\eta), \quad (46)$$

$$\phi_{\mathrm{tot}}(\boldsymbol{\zeta},\eta,k_2) = c_\alpha(\boldsymbol{\zeta},\eta)\psi_\alpha(\boldsymbol{\zeta},\eta) + c_D(\boldsymbol{\zeta},\eta,k_2)\psi_D(\boldsymbol{\zeta},\eta), \quad (47)$$

which can be easily solved for ψ_α and ψ_D. Therefore the functions ψ_α and ψ_D can be found separately for all values of $\boldsymbol{\zeta}$ and η and the absorption and diffusion coefficients—by the inverse Fourier-Laplace transformation of these functions. In particular, we obtain from Eqs. (46) and (47) and Eqs. (44) and (45)

$$\psi_\alpha(\boldsymbol{\zeta},\eta) = \frac{(D_0\eta)^2}{k_1^2-k_2^2}\{k_1^2\phi_{\mathrm{tot}}(\boldsymbol{\zeta},\eta,k_2) - k_2^2\phi_{\mathrm{tot}}(\boldsymbol{\zeta},\eta,k_1) + (\eta^2/2 - \zeta^2/2)[\phi_{\mathrm{tot}}(\boldsymbol{\zeta},\eta,k_1) - \phi_{\mathrm{tot}}(\boldsymbol{\zeta},\eta,k_2)]\}, \quad (48)$$

$$\psi_D(\boldsymbol{\zeta},\eta) = (D_0\eta)^2\frac{\phi_{\mathrm{tot}}(\boldsymbol{\zeta},\eta,k_2) - \phi_{\mathrm{tot}}(\boldsymbol{\zeta},\eta,k_1)}{k_1^2-k_2^2}. \quad (49)$$

D. Reconstruction in the Biplanar Geometry

Now we briefly discuss the case in which the sources and detectors are placed on different planes. Without loss of generality, we can assume that $z_s = 0$, $z_d = L$, and $0 < z < L$. We consider first the reconstruction of the absorption ($\delta D = 0$ and $\delta\alpha \neq 0$). Equation (17) now assumes the form

$$\phi_\alpha(\mathbf{q}_1,\mathbf{q}_2) = \frac{\exp[-LQ(q_2)]}{(2D_0)^2 Q(q_1)Q(q_2)}\int d^2\rho\mathrm{d}z\,\delta\alpha(\boldsymbol{\rho},z) \times \exp\{i(\mathbf{q}_1+\mathbf{q}_2)\cdot\boldsymbol{\rho} - [Q(q_1)-Q(q_2)]z\}. \quad (50)$$

Again, we use the new variables [Eqs. (21)–(23)], but now we restrict consideration to the subspace defined by $\eta_1 = -\eta_2 = \eta$. Substituting the new variables into Eq. (50), we obtain an equation that has exactly the same form as Eq. (26), but with ψ defined by

$$\psi_\alpha(\boldsymbol{\zeta},\eta) = -(D_0\eta)^2\exp(-\eta L/2)\phi_\alpha[\mathbf{q}_1(\boldsymbol{\zeta},\eta),\mathbf{q}_2(\boldsymbol{\zeta},\eta)]. \quad (51)$$

It is important to note that measurements in the biplanar geometry are more suitable for numerical inversion than in the single-plane geometry. Mathematically, this follows from the fact that there is a minus sign in the exponential factor $[Q(q_1)-Q(q_2)]z$ in Eq. (50) [compare with Eq. (20)], and the Laplace transform of $\delta\alpha$ can be obtained for smaller values of the Laplace variable without analytic continuation. Physically, this can be interpreted by observing that in the case of the biplanar geometry, the photons that propagate from the plane $z = z_s$ to the plane $z = z_d$ are more likely to cross the region where $\delta\alpha \neq 0$ than the photons that were emitted and detected on the same plane.

For the reconstruction of the diffusion coefficient ($\delta\alpha = 0$ and $\delta D \neq 0$), we obtain

$$\phi_D(\mathbf{q}_1,\mathbf{q}_2) = \frac{-\exp[-LQ(q_1)][Q(q_1)Q(q_2)+\mathbf{q}_1\cdot\mathbf{q}_2]}{(2D_0)^2 Q(q_1)Q(q_2)} \times \int \mathrm{d}^2\rho\mathrm{d}z\,\delta\alpha(\boldsymbol{\rho},z)\exp[i(\mathbf{q}_1+\mathbf{q}_2)\cdot\boldsymbol{\rho} - (Q(q_1)-Q(q_2))z]. \quad (52)$$

With the same transformation of variables as above, this can be brought to the form (39) with the function ψ given by

$$\psi_D(\boldsymbol{\zeta},\eta) = \frac{-(D_0\eta)^2\exp(-\eta L/2)\phi_D[\mathbf{q}_1(\boldsymbol{\zeta},\eta),\mathbf{q}_2(\boldsymbol{\zeta},\eta)]}{(\eta^2 - \zeta^2 - 2k^2)}. \quad (53)$$

Finally, in the case when both $\delta\alpha$ and δD are not zero, we can use the two-frequency method described in Subsection 3.C. The only difference is that the expressions for the coefficients c_α and c_D on the right-hand side of Eqs. (44) and (45) must be multiplied by an extra factor of $-\exp(\eta L/2)$, as follows from Eqs. (51) and (53).

E. Reconstruction with a Fixed Source

To conclude the discussion of the planar geometry, we consider reconstruction from measurements with a fixed source. We assume that the location of the source on the measurement plane, $\boldsymbol{\rho}_1$, is fixed, while the detectors, $\boldsymbol{\rho}_2$, can still occupy the measurement plane. Thus the data function with a fixed source has only two degrees of freedom, and the inverse problem is underdetermined. However, we can add an additional degree of freedom by varying the modulation frequency ω or the wave number k, which makes the data three-dimensional. In this subsection we consider only reconstruction of the absorption coefficient; the derivations for the diffusion coefficient can be easily carried out as described in Subsection 3.B.

Without loss of generality, we set $\boldsymbol{\rho}_1 = 0$. The data function in this case depends on $\boldsymbol{\rho}_2$ and k:

$$\phi_\alpha(\boldsymbol{\rho}_2, k) = \frac{1}{(2\pi)^3 D_0} \int \mathrm{d}^3 r\, \delta\alpha(\mathbf{r}) G_0(\mathbf{r}, 0) \times \int \mathrm{d}^3 p\, \frac{\exp[i\mathbf{p}\cdot(\boldsymbol{\rho}_1 - \mathbf{r})]}{p^2 + k^2}, \tag{54}$$

where we have used the expansion (12). Since $G_0(\mathbf{r}, 0)$ depends only on $\mathbf{r}$ we can consider the combination $a(\mathbf{r}) = \delta\alpha(\mathbf{r}) G_0(\mathbf{r}, 0)$ as the unknown function to be reconstructed.

Following the general procedure outlined in Subsection 3.A, we Fourier transform $\phi_\alpha(\boldsymbol{\rho}_2, k)$ according to

$$\phi_\alpha(\mathbf{q}, k) = \int \phi_\alpha(\boldsymbol{\rho}_1, k) \exp(i\mathbf{q}\cdot\boldsymbol{\rho}_1) \mathrm{d}^2\rho_1 \tag{55}$$

to obtain (in the case $z_s = z_d = 0$ and $z > 0$)

$$\phi_\alpha(\mathbf{q}, k) = \frac{1}{2D_0} \int \mathrm{d}^3 r a(\mathbf{r}) \frac{\exp[i\mathbf{q}\cdot\boldsymbol{\rho} - zQ(q)]}{Q(q)}. \tag{56}$$

Next, we introduce new variables, $\boldsymbol{\zeta}$ and η, according to

$$\boldsymbol{\zeta} = \mathbf{q}, \tag{57}$$

$$\eta = Q(q). \tag{58}$$

This transformation is obviously invertible. In the new variables we have

$$\psi_\alpha(\boldsymbol{\zeta}, \eta) = \int \mathrm{d}^2\rho \mathrm{d}z\, a(\boldsymbol{\rho}, z) \exp(i\boldsymbol{\zeta}\cdot\boldsymbol{\rho} - \eta z), \tag{59}$$

where $\psi_\alpha(\boldsymbol{\zeta}, \eta) = \phi_\alpha[\mathbf{q}(\boldsymbol{\zeta}, \eta), k(\boldsymbol{\zeta}, \eta)]$, and $\mathbf{q}(\boldsymbol{\zeta}, \eta) = \boldsymbol{\zeta}$, $k(\boldsymbol{\zeta}, \eta) = (\eta^2 - \zeta^2)^{1/2}$.

As can be seen from definition (4), the variable k^2 can vary in the complex plane along the semi-infinite line $[k_0^2 - i0, k_0^2 - i\infty)$ where $k_0^2 = \alpha_0/D_0$. From this line the data function can be analytically continued to arbitrary complex values of k^2, and Eq. (59) can be solved for $a(\mathbf{r})$ by the inverse Fourier–Laplace transformation.

This proves that measurements with a fixed source but multiple modulation frequencies can also be used for the reconstruction of the absorption coefficient when there are no fluctuations in the diffusion coefficient. It is also possible to reconstruct the diffusion coefficients in this setting when there are no fluctuations in the absorption coefficient. Simultaneous reconstruction of $\delta\alpha$ and δD is not possible with a single fixed source. It is, however, plausible that such reconstructions can be carried out with two fixed spatially separated sources.

4. CYLINDRICAL GEOMETRY

In this section we assume that the sources and detectors are located on the surface of an infinite cylinder of radius R (Fig. 1). The functions $\delta\alpha(\rho, \varphi, z)$ and $\delta D(\rho, \varphi, z)$ are taken to vanish for $\rho > R$. In cylindrical coordinates, the data function can be written as $\phi = \phi(\varphi_1, z_1; \varphi_2, z_2)$, since the value of the coordinate ρ is fixed for both sources and detectors. First, we discuss reconstruction of $\delta\alpha$ and δD separately. Given the reconstruction formulas for $\delta\alpha \neq 0$, $\delta D = 0$ and $\delta D \neq 0$, $\delta\alpha = 0$, simultaneous reconstruction of these two functions is carried out as discussed in Subsection 3.C.

A. Reconstruction of the Absorption Coefficient

We start by considering the case $\delta D = 0$ and $\delta\alpha \neq 0$. Using expansion (13) and the cylindrical reference frame $\mathbf{r} = (\rho, \varphi, z)$, we can write

$$\begin{aligned}\phi_\alpha(\varphi_1, z_1; \varphi_2, z_2) &= \frac{1}{(2\pi)^4 D_0^2} \sum_{m_1, m_2 = -\infty}^{\infty} \exp[-i(m_1\varphi_1 - m_2\varphi_2)] \\ &\times \int_{-\infty}^{\infty} \mathrm{d}q_1 \int_{-\infty}^{\infty} \mathrm{d}q_2 \exp[i(q_1 z_1 - q_2 z_2)] \\ &\times K_{m_1}(RQ(q_1)) K_{m_2}(RQ(q_2)) \\ &\times \int \mathrm{d}^3 r\, \delta\alpha(\mathbf{r}) \exp\{i[(m_2 - m_1)\varphi + (q_2 - q_1)z]\} \\ &\times I_{m_1}(\rho Q(q_1)) I_{m_2}(\rho Q(q_2)),\end{aligned} \tag{60}$$

where $Q(q)$ is given by Eq. (18). Now we Fourier transform the data according to

$$\begin{aligned}\phi_\alpha(m_1, q_1; m_2, q_2; \tilde{\varphi}) &= \int_{-\infty}^{\infty} \mathrm{d}z_1 \int_{-\infty}^{\infty} \mathrm{d}z_2 \int_0^{2\pi} \mathrm{d}\varphi_1 \int_0^{2\pi} \mathrm{d}\varphi_2 \phi_\alpha(\varphi_1, z_1; \varphi_2, z_2) \\ &\times \exp\{i[q_1 z_1 + q_2 z_2 + m_1(\varphi_1 - \tilde{\varphi}) \\ &+ m_2(\varphi_2 - \tilde{\varphi})]\},\end{aligned} \tag{61}$$

where $\tilde{\varphi}$ is an arbitrary polar angle defined in the laboratory frame. Applying Eq. (61) to Eq. (60), we obtain

$$\phi_\alpha(m_1, q_1; m_2, q_2; \tilde{\varphi}) = \frac{\exp[-i(m_1 + m_2)\tilde{\varphi}]}{(2\pi)^4 D_0^2} K_{m_1}(RQ(q_1)) K_{m_2}(RQ(q_2)) \times \int \mathrm{d}^3 r\, \delta\alpha(\mathbf{r}) \exp[i(q_1 + q_2)z + i(m_1 + m_2)\varphi] \times I_{m_1}(\rho Q(q_1)) I_{m_2}(\rho Q(q_2)). \quad (62)$$

Now we define a new data function by

$$\psi_\alpha(q_1, q_2; \tilde{\varphi}) = \sum_{m_1, m_2 = -\infty}^{\infty} \frac{(2\pi)^4 D_0^2 \phi_\alpha(m_1, q_1; m_2, q_2; \tilde{\varphi})}{K_{m_1}(RQ(q_1)) K_{m_2}(RQ(q_2))} \quad (63)$$

and use the equality

$$\sum_{m=-\infty}^{\infty} I_m(w) \exp(im\theta) = \exp(w \cos\theta) \quad (64)$$

to show that

$$\psi_\alpha(q_1, q_2; \tilde{\varphi}) = \int \mathrm{d}^3 r\, \delta\alpha(\mathbf{r}) \exp[i(q_1 + q_2)z + \boldsymbol{\rho} \cdot \hat{\mathbf{e}}(Q(q_1) + Q(q_2))], \quad (65)$$

where $\hat{\mathbf{e}}$ is the unit vector perpendicular to the cylinder axis and is characterized by the polar angle $\tilde{\varphi}$.

As in the case of the planar geometry, Eq. (65) resembles the Fourier–Laplace transform of $\delta\alpha$. Following the main idea of Section 3, we introduce new variables η and ζ according to

$$\eta = q_1 + q_2, \quad (66)$$

$$\boldsymbol{\zeta} = (Q(q_1) + Q(q_2))\hat{\mathbf{e}}. \quad (67)$$

Here $\boldsymbol{\zeta}$ is a two-dimensional vector perpendicular to the cylinder axis. The transformation is invertible and maps the three-dimensional manifold determined by $(q_1, q_2, \hat{\mathbf{e}})$ onto the three-dimensional manifold of $(\eta, \boldsymbol{\zeta})$. The Jacobian is given by

$$J = \frac{\partial(\eta, \boldsymbol{\zeta})}{\partial(q_1, q_2, \hat{\mathbf{e}})} = \left[\frac{q_2}{Q(q_2)} - \frac{q_1}{Q(q_1)}\right][Q(q_1) + Q(q_2)] \quad (68)$$

and vanishes only when $q_1 = q_2$. The solution of Eqs. (66) and (67) for q_1, q_2 has the form

$$q_{1,2} = \left[\frac{\eta^4 + 4k^2\zeta^2 - \zeta^4}{4(\eta^2 - \zeta^2)} \pm \frac{\eta\zeta}{2}\left(\frac{4k^2}{\eta^2 - \zeta^2} + 1\right)^{1/2}\right]^{1/2}, \quad (69)$$

and the direction of the unit vector $\hat{\mathbf{e}}$ coincides with that of $\boldsymbol{\zeta}$ (note that $\boldsymbol{\zeta}$ is guaranteed to have a definite direction, since its complex Cartesian components have the same phase). In the new variables, integral equation (63) has the form

$$\psi_\alpha(\eta, \boldsymbol{\zeta}) = \int \mathrm{d}^3 r\, \delta\alpha(\mathbf{r}) \exp(i\eta z + \boldsymbol{\zeta} \cdot \boldsymbol{\rho}), \quad (70)$$

which can be formally inverted as was described in Section 3. Note that in the case of cylindrical geometry the Laplace part of the inverse transformation is two dimensional (it is one dimensional in the planar geometry).

As in the case of planar geometry, inversion of Eq. (70) requires an analytic continuation of the Fourier-transformed data function to complex values of q_1 and q_2. The inversion kernel can be written as

$$K_\alpha(\boldsymbol{\rho}, z; \varphi_1, z_1, \varphi_2, z_2) = -2\pi D_0^2 \sum_{m_1, m_2 = -\infty}^{\infty} \exp[i(m_1\varphi_1 + m_2\varphi_2)] \int_{-\infty}^{\infty} \mathrm{d}\eta \exp(-i\eta z) \times \int \mathrm{d}^2\zeta \frac{\exp[-\boldsymbol{\zeta} \cdot \boldsymbol{\rho} - i(m_1 + m_2)\tilde{\varphi} + i(q_1 z_1 + q_2 z_2)]}{K_{m_1}(RQ(q_1)) K_{m_2}(RQ(q_2))}, \quad (71)$$

where $\tilde{\varphi}$ is the angle between $\boldsymbol{\zeta}$ and $\boldsymbol{\rho}$, and the variables q_1, q_2 must be expressed in terms of ζ and η according to Eq. (69).

The reconstruction described in this section employs a transformation of the data function that depends on a unit vector $\hat{\mathbf{e}}$ (which is determined by the polar angle $\tilde{\varphi}$). It is important to emphasize that $\tilde{\varphi}$ can be varied from 0 to 2π. One can also develop an approach in which the reconstruction procedure utilizes two mathematically independent unit vectors (see subsection 4.D). In the case of the spherical geometry discussed below (Section 5) two unit vectors are *required* for the reconstruction procedure.

B. Reconstruction of the Diffusion Coefficient

We proceed with the reconstruction of the diffusion coefficient by rewriting Eq. (11) with $\delta\alpha = 0$ and using representation (13) for the Green's functions in cylindrical coordinates. The analog of Eq. (60) is

$$\phi_D(\varphi_1, z_1; \varphi_2, z_2) = \frac{1}{(2\pi)^4 D_0^2} \sum_{m_1, m_2 = -\infty}^{\infty} \exp[i(m_1\varphi_1 - m_2\varphi_2)] \times \int_{-\infty}^{\infty} \mathrm{d}q_1 \int_{-\infty}^{\infty} \mathrm{d}q_2 \exp[i(q_1 z_1 - q_2 z_2)] \times K_{m_1}(RQ(q_1)) K_{m_2}(RQ(q_2)) \int \mathrm{d}^3 r\, \delta D(\mathbf{r}) \times [\nabla_{\mathbf{r}} \exp[-i(q_1 z + m_1\varphi)] I_{m_1}(\rho Q(q_1))] \cdot [\nabla_{\mathbf{r}} \exp[i(q_2 z + m_2\varphi)] I_{m_2}(\rho Q(q_2))]. \quad (72)$$

After Fourier transformation using Eq. (61), this becomes

$$\phi_D(m_1, q_1; m_2, q_2; \tilde{\varphi}) = (2\pi)^4 D_0^2 \exp[-i(m_1 + m_2)\tilde{\varphi}] \times K_{m_1}(RQ(q_1))K_{m_2}(RQ(q_2)) \times \int d^3r\, \delta\alpha(\mathbf{r})\{\nabla_{\mathbf{r}} \exp[i(q_1 z + m_1\varphi)]I_{m_1}(\rho Q(q_1))\} \cdot \{\nabla_{\mathbf{r}} \exp[i(q_2 z + m_2\varphi)]I_{m_2}(\rho Q(q_2))\}. \quad (73)$$

Now we define the new data function ψ_D according to Eq. (63) and use Eq. (64) to obtain

$$\psi_D(q_1, q_2; \tilde{\varphi}) = \int d^3r\, \delta D(\mathbf{r})[\nabla_{\mathbf{r}} \exp(iq_1 z + \boldsymbol{\rho} \cdot \hat{\mathbf{e}} Q(q_1))] \cdot [\nabla_{\mathbf{r}} \exp(iq_2 z + \boldsymbol{\rho} \cdot \hat{\mathbf{e}} Q(q_2))]. \quad (74)$$

At this point, the action of the gradient operators can be easily evaluated. The result is

$$\psi_D(q_1, q_2; \tilde{\varphi}) = [Q(q_1)Q(q_2) - q_1 q_2] \times \int d^3r\, \delta D(\mathbf{r}) \exp\{i(q_1 + q_2)z + [Q(q_1) + Q(q_2)]\hat{\mathbf{e}} \cdot \boldsymbol{\rho}\}. \quad (75)$$

In the new variables defined by Eqs. (66) and (67), this equation can be rewritten as

$$\psi_D(\eta, \boldsymbol{\zeta}) = \frac{\zeta^2 - \eta^2 - 2k^2}{2} \int d^3r\, \delta D(\mathbf{r}) \exp(i\eta z + \boldsymbol{\zeta} \cdot \boldsymbol{\rho}), \quad (76)$$

where we have used

$$Q(q_1)Q(q_2) - q_1 q_2 = \frac{\zeta^2 - \eta^2 - 2k^2}{2}, \quad (77)$$

which can be directly derived from Eq. (69).

The reconstruction of δD can be carried out by applying the inverse Fourier–Laplace transform to the function $2\psi_D/(\zeta^2 - \eta^2 - 2k^2)$. The inversion kernel is given by Eq. (71), where the integrand must be multiplied by the additional factor $2/(\zeta^2 - \eta^2 - 2k^2)$.

C. Simultaneous Reconstruction of $\delta\alpha$ and δD

In the case when both $\delta\alpha$ and δD are nonzero, the data function is defined by the general equation (11). We define the function ψ_{tot} by analogy to Eq. (63):

$$\psi_{\text{tot}}(q_1, q_2; \tilde{\varphi}) = \sum_{m_1, m_2 = -\infty}^{\infty} \frac{(2\pi)^4 D_0^2 \phi_{\text{tot}}(m_1, q_1; m_2, q_2; \tilde{\varphi})}{K_{m_1}(RQ(q_1))K_{m_2}(RQ(q_2))}. \quad (78)$$

Combining the derivations of Subsections 4.A and 4.B, we can see that

$$\psi_{\text{tot}}(\eta, \boldsymbol{\zeta}, k) = \int d^3r[\delta\alpha(\mathbf{r}) + c(\eta, \zeta, k)\delta D(\mathbf{r})] \times \exp(i\eta z + \boldsymbol{\zeta} \cdot \boldsymbol{\rho}), \quad (79)$$

where $c(\eta, \zeta, k) = k^2(\zeta^2 + \eta^2)/(\zeta^2 - \eta^2)$ and we have indicated the *explicit* dependence on k. It is important that $\delta\alpha$ and δD in Eq. (79) do not depend on k explicitly. As was discussed in Subsection 3.C, we can treat η, $\boldsymbol{\zeta}$, and k as mathematically independent variables and use two different modulation frequencies to obtain a system of equations for $\delta\alpha$ and δD. These equations can be solved for every pair of values η and $\boldsymbol{\zeta}$, and thus $\delta\alpha$ and δD can be reconstructed with the inverse Fourier–Laplace transform.

D. Reconstruction with Two Unit Vectors in the Cylindrical Geometry

It is possible to develop an approach slightly different from the one described in Subsections 4.A–4.C. That is we introduce two different and mathematically independent polar angles, $\tilde{\varphi}_1$ and $\tilde{\varphi}_2$, and two corresponding unit vectors, $\hat{\mathbf{e}}_1$ and $\hat{\mathbf{e}}_2$. Instead of Eq. (61), we define the Fourier-transformed data function according to

$$\phi_\alpha(m_1, q_1; m_2, q_2; \tilde{\varphi}_1, \tilde{\varphi}_2) = \int_{-\infty}^{\infty} dz_1 \int_{-\infty}^{\infty} dz_2 \int_0^{2\pi} d\varphi_1 \int_0^{2\pi} d\varphi_2 \phi_\alpha(\varphi_1, z_1; \varphi_2, z_2) \times \exp\{i[q_1 z_1 + q_2 z_2 + m_1(\varphi_1 - \tilde{\varphi}_1) + m_2(\varphi_2 - \tilde{\varphi}_2)]\}. \quad (80)$$

This leads to the following expression for ψ_α, which is now a function of $q_1, q_2, \tilde{\varphi}_1, \tilde{\varphi}_2$:

$$\psi_\alpha(q_1, q_2; \tilde{\varphi}_1, \tilde{\varphi}_2) = \int d^3r\, \delta\alpha(\mathbf{r}) \exp[i(q_1 + q_2)z + \boldsymbol{\rho} \cdot (\hat{\mathbf{e}}_1 Q(q_1) + \hat{\mathbf{e}}_2 Q(q_2))]. \quad (81)$$

Now we introduce new variables, η and $\boldsymbol{\zeta}$, similar to the those in Eqs. (66) and (67):

$$\eta = q_1 + q_2, \quad (82)$$

$$\boldsymbol{\zeta} = \hat{\mathbf{e}}_1 Q(q_1) + \hat{\mathbf{e}}_2 Q(q_2). \quad (83)$$

The above transformation maps the four-dimensional manifold $(q_1, q_2, \hat{\mathbf{e}}_1, \hat{\mathbf{e}}_2)$ onto a three-dimensional manifold $(\eta, \boldsymbol{\zeta})$ and is not uniquely invertible. The results in Subsections 4.A–4.C were obtained by restricting attention to the three dimensional submanifold defined by $\hat{\mathbf{e}}_1 = \hat{\mathbf{e}}_2 = \hat{\mathbf{e}}$. Another approach, which we discuss in this subsection, is to let $\hat{\mathbf{e}}_1$ and $\hat{\mathbf{e}}_2$ be independent and require instead that $q_1 = q_2 = q$. This leads to

$$\eta = 2q, \quad (84)$$

$$\boldsymbol{\zeta} = Q(q)(\hat{\mathbf{e}}_1 + \hat{\mathbf{e}}_2). \quad (85)$$

Using the above definitions of η and $\boldsymbol{\zeta}$, we will invert Eq. (70). For this purpose, $\psi_\alpha(\eta, \boldsymbol{\zeta})$ must be evaluated for η's varying along the real axis and the Cartesian components of $\boldsymbol{\zeta}$ along the imaginary axis. The first is easily achieved because $q_{1,2}$ in Eq. (61) can vary from $-\infty$ to ∞. However, as follows from Eq. (85), the second condition cannot be achieved because $\hat{\mathbf{e}}_{1,2}$ are by definition unit vectors with real components, and analytic continuation of the data function to complex values of $\hat{\mathbf{e}}_{1,2}$ is problematic. Instead, the Laplace transform can be inverted by discretizing the transformed function and mapping the integral equation onto a system of linear algebraic equations.

5. SPHERICAL GEOMETRY

For the spherical geometry, sources and detectors are located on the surface of a sphere of radius R. The data function depends on the azimuthal and polar angles θ and φ of the sources and detectors. Equivalently, we can view the data function as a function of two unit vectors, $\hat{\mathbf{r}}_1$ and $\hat{\mathbf{r}}_2$, pointing in the direction of sources and detectors, respectively.

A. Reconstruction of the Absorption Coefficient

Using representation (14) of G_0, we can write the data function in the case $\delta D = 0$:

$$\phi_\alpha(\hat{\mathbf{r}}_1, \hat{\mathbf{r}}_2) = \left(\frac{k}{2\pi^2 D_0}\right)^2 \sum_{l_1, l_2=0}^{\infty} (2l_1+1)(2l_2+1) k_{l_1}(kR) k_{l_2}(kR) \times \int \mathrm{d}^3 r\, \delta\alpha(\mathbf{r}) i_{l_1}(kr) i_{l_2}(kr) P_{l_1}(\hat{\mathbf{r}}\cdot\hat{\mathbf{r}}_1) P_{l_2}(\hat{\mathbf{r}}\cdot\hat{\mathbf{r}}_1). \tag{86}$$

The analog of the Fourier transformation of the data function defined on a sphere is integration with respect to the function $P_{l_1}(\hat{\mathbf{e}}_1\cdot\hat{\mathbf{r}}_1)P_{l_2}(\hat{\mathbf{e}}_2\cdot\hat{\mathbf{r}}_2)$, where $\hat{\mathbf{e}}_1$, $\hat{\mathbf{e}}_2$ are two arbitrary unit vectors. The transformation of the ϕ function is defined by

$$\phi_\alpha(l_1, l_2; \hat{\mathbf{e}}_1, \hat{\mathbf{e}}_2) = \int \phi_\alpha(\hat{\mathbf{r}}_1, \hat{\mathbf{r}}_2) P_{l_1}(\hat{\mathbf{e}}_1\cdot\hat{\mathbf{r}}_1) \times P_{l_2}(\hat{\mathbf{e}}_2\cdot\hat{\mathbf{r}}_2)\mathrm{d}\Omega_1\mathrm{d}\Omega_2, \tag{87}$$

where $\mathrm{d}\Omega_{1,2}$ is an element of solid angle in the direction of the corresponding unit vector.

Applying transformation (87) to data function (86) and using the orthogonality of Legendre polynomials in the form

$$\int P_{l_1}(\hat{\mathbf{a}}\cdot\hat{\mathbf{x}}) P_{l_2}(\hat{\mathbf{b}}\cdot\hat{\mathbf{x}})\mathrm{d}\Omega_{\hat{x}} = \frac{4\pi\delta_{l_1 l_2}}{2l_1+1} P_{l_1}(\hat{\mathbf{a}}\cdot\hat{\mathbf{b}}), \tag{88}$$

we obtain

$$\phi_\alpha(l_1, l_2; \hat{\mathbf{e}}_1, \hat{\mathbf{e}}_2) = \left(\frac{2k}{\pi D_0}\right)^2 k_{l_1}(kR) k_{l_2}(kR) \times \int \mathrm{d}^3 r\, \delta\alpha(\mathbf{r}) i_{l_1}(kr) i_{l_2}(kr) P_{l_1}(\hat{\mathbf{r}}\cdot\hat{\mathbf{e}}_1) P_{l_2}(\hat{\mathbf{r}}\cdot\hat{\mathbf{e}}_2). \tag{89}$$

Next, we use the plane wave expansion in the form

$$\exp(\mathbf{a}\cdot\mathbf{b}) = \sum_{l=0}^{\infty} (2l+1) i_l(ab) P_l(\hat{\mathbf{a}}\cdot\hat{\mathbf{b}}) \tag{90}$$

and define the new data function as

$$\psi_\alpha(\hat{\mathbf{e}}_1, \hat{\mathbf{e}}_2) = \sum_{l_1, l_2=0}^{\infty} \left(\frac{\pi D_0}{2k}\right)^2 \times \frac{(2l_1+1)(2l_2+1)\phi_\alpha(l_1, l_2; \hat{\mathbf{e}}_1, \hat{\mathbf{e}}_2)}{k_{l_1}(kR) k_{l_2}(kR)}. \tag{91}$$

It readily follows from Eq. (90) and application of the transformation (91) to the data function (89) that

$$\psi_\alpha(\hat{\mathbf{e}}_1, \hat{\mathbf{e}}_2) = \int \mathrm{d}^3 r\, \delta\alpha(\mathbf{r}) \exp[k(\hat{\mathbf{e}}_1 + \hat{\mathbf{e}}_2)\cdot\mathbf{r}]. \tag{92}$$

The above equation has the form of a three-dimensional Laplace transform of the absorption coefficient $\delta\alpha$. As in the case of the cylindrical geometry with two unit vectors discussed in Subsection 4.D, analytic continuation to complex values of $\boldsymbol{\zeta} = k(\hat{\mathbf{e}}_1 + \hat{\mathbf{e}}_2)$, which is necessary for analytic inversion of Eq. (92), is problematic. For this reason, we are not able to write an analytic expression for the inversion kernel. However, numerical inversion of Eq. (92) is quite feasible.

B. Reconstruction of the Diffusion Coefficient

The reconstruction of the diffusion coefficient is easily achieved by following the general procedures outlined in the previous sections. Again, we perform all the transformations of Subsection 5.A, retaining the gradient operators under the integral, and calculate the action of the latter at the last stage. In particular, the expression for ψ_D becomes

$$\psi_D(\hat{\mathbf{e}}_1, \hat{\mathbf{e}}_2) = \int \mathrm{d}^3 r\, \delta D(\mathbf{r}) [\nabla_{\mathbf{r}} \exp(k\hat{\mathbf{e}}_1\cdot\mathbf{r})]\cdot[\nabla_{\mathbf{r}} \exp(k\hat{\mathbf{e}}_2\cdot\mathbf{r})], \tag{93}$$

which is easily evaluated and yields

$$\psi_D(\hat{\mathbf{e}}_1, \hat{\mathbf{e}}_2) = k^2(\hat{\mathbf{e}}_1\cdot\hat{\mathbf{e}}_2)\int \mathrm{d}^3 r\, \delta D(\mathbf{r}) \exp[k(\hat{\mathbf{e}}_1 + \hat{\mathbf{e}}_2)\cdot\mathbf{r}]. \tag{94}$$

Equation (94) is similar to Eq. (92), except that $\psi_\alpha(\hat{\mathbf{e}}_1, \hat{\mathbf{e}}_2)$ is replaced by $\psi_D(\hat{\mathbf{e}}_1, \hat{\mathbf{e}}_2)/k^2(\hat{\mathbf{e}}_1\cdot\hat{\mathbf{e}}_2)$, and all the arguments at the end of Subsection 5.A apply.

C. Simultaneous reconstruction of $\delta\alpha$ and δD

To carry out simultaneous reconstruction of $\delta\alpha$ and δD we must find the two integrals containing $\delta\alpha$ and δD from the equation for the total data function:

$$\psi_{\mathrm{tot}}(\hat{\mathbf{e}}_1, \hat{\mathbf{e}}_2) = \int \mathrm{d}^3 r [\delta\alpha(\mathbf{r}) + k^2(\hat{\mathbf{e}}_1\cdot\hat{\mathbf{e}}_2)\delta D(\mathbf{r})] \times \exp[k(\hat{\mathbf{e}}_1 + \hat{\mathbf{e}}_2)\cdot\mathbf{r})]. \tag{95}$$

In principle, this can be achieved by considering two modulation frequencies and viewing the coefficient $k^2(\hat{\mathbf{e}}_1\cdot\hat{\mathbf{e}}_2)$ as explicitly depending on k. However, the implicit dependence of the integrands on k is suppressed only if we perform two measurements for $(k, \hat{\mathbf{e}}_1, \hat{\mathbf{e}}_2)$ and $(k', \hat{\mathbf{e}}_1', \hat{\mathbf{e}}_2')$ such that $k(\hat{\mathbf{e}}_1 + \hat{\mathbf{e}}_2) = k'(\hat{\mathbf{e}}_1' + \hat{\mathbf{e}}_2')$, thus keeping the variable $\boldsymbol{\zeta}$ constant. This is possible if the

complex numbers k and k' have the same phase and $\hat{\mathbf{e}}_1 + \hat{\mathbf{e}}_2$ and $\hat{\mathbf{e}}_1' + \hat{\mathbf{e}}_2'$ have the same direction. But as follows from definition (4) varying the modulation frequency changes the phase of k. Therefore the data function for two different values of k with the same complex phase can be obtained only by analytic continuation, as described in Subsection 3.E. This in turn requires measurements with multiple modulation frequencies. Therefore unlike in the cases of the planar and the cylindrical geometries, simultaneous reconstruction of $\delta\alpha$ and δD in the spherical geometry requires measurements with many different modulation frequencies rather than just two.

6. DISCUSSION

In this paper we have demonstrated that the inverse problem of reconstructing the absorption and diffusion coefficients of a highly scattering medium probed by diffuse light has a unique solution. The derivations were performed without consideration of boundary conditions in three different geometries. In all cases the data function, determined as a function of the locations of the sources and the detectors, has four degrees of freedom, whereas the reconstructed functions have only three degrees of freedom. This makes the problem overdetermined, and, as is well known from the theory of linear operators, the existence of a *unique* solution is not guaranteed in this case. However, we have shown that it is possible to restrict the domain of the data function to a three-dimensional manifold in such a way that a certain uniquely defined transformation of the experimentally measurable data function becomes the Fourier–Laplace transform of the function that is to be reconstructed. This fact guarantees that the quantity to be reconstructed is uniquely defined by this restriction of the data function, provided that the data are physically admissible.

Inversion formulas based on the Fourier–Laplace transform were derived. These formulas were verified for pointlike absorbers and scatterers. However, their numerical stability, especially in the presence of noise, has to be further investigated. The results also have practical significance for the interpretation of inversion formulas based on singular-value decomposition, which are better suited for numerical work but do not guarantee that the obtained result will coincide with the true solution.

It is interesting to note that the Laplace part of the inverse Fourier–Laplace transformation is one dimensional in the case of planar geometry, two dimensional in the case of the cylindrical geometry, and three dimensional for the spherical geometry. This fact can be easily interpreted geometrically: In the case of the planar geometry the Fourier part of transformation is associated with the longitudinal (two-dimensional) coordinates and the Laplace transformation is associated with the transverse coordinate; in the case of the cylindrical geometry the Fourier transformation is associated with the cylinder axis; and, finally, in the case of spherical geometry, there is no Fourier part. Thus the Fourier part of the transformation is associated with the directions in space that have translational invariance in the absence of inhomogeneities. Since the Laplace transform is known to be numerically unstable, we can conclude that the computationally preferable geometrical setting is planar.

The results of numerical calculations will be presented in the third paper in this series. The most serious problem in practical application of the formulas derived here is numerical inversion of the Laplace transform. A number of methods for such inversion have been employed in different areas of physics.[36–40] Typically, some *a priori* knowledge about the reconstructed function is required to make the inversion numerically stable. In Part III of this series we will present a method based on singular-value decomposition that does not require such knowledge and is numerically stable in the presence of noise.

ACKNOWLEDGMENT

The authors are grateful to P. S. Carney for very useful discussions. This research was supported by the National Institutes of Health under the grant 2P41-02305-16.

V. A. Markel and J. C. Schotland can be reached via e-mail at vmarkel@ee.wustl.edu and jcs@ee.wustl.edu, respectively.

REFERENCES AND NOTES

1. G. Mueller, ed., *Medical Optical Tomography: Functional Imaging and Monitoring* (SPIE Press, Bellingham, Wash., 1993).
2. R. Alfano, ed., *Advances in Optical Imaging and Photon Migration* (Optical Society of America, Washington, D.C., 1994).
3. B. Chance and R. Alfano, eds., *Proceedings of Optical Tomography and Spectroscopy of Tissue* (SPIE Press, Bellingham, Wash., 1995).
4. B. Chance and R. Alfano, eds., *Proceedings of Optical Tomography and Spectroscopy of Tissue II* (SPIE Press, Bellingham, Wash., 1997).
5. B. Chance, R. Alfano, and B. Tromberg, eds., *Proceedings of Optical Tomography and Spectroscopy of Tissue III* (SPIE Press, Bellingham, Wash., 1999).
6. M. C. W. van Rossum and T. M. Nieuwenhuizen, "Multiple scattering of classical waves: microscopy, mesoscopy, and diffusion," Rev. Mod. Phys. **71**, 313–371 (1999).
7. A. B. Davis, R. F. Cahalan, D. Spinehirne, M. J. McGill, and S. P. Love, "Off-beam lidar: an emerging technique in cloud remote sensing based on radiative Green-function theory in the diffusion domain," Phys. Chem. Earth B **24**, 177–185 (1999).
8. L. Wang, P. P. Ho, C. Liu, G. Zhang, and R. R. Alfano, "Ballistic 2-D imaging through scattering walls using an ultrafast optical Kerr gate," Science **253**, 769–771 (1991).
9. D. A. Benaron and D. K. Stevenson, "Optical time-of-flight and absorbance imaging of biologic media," Science **259**, 1463–1466 (1993).
10. A. Rebane and J. Feinberg, "Time-resolved holography," Nature **351**, 378–380 (1991).
11. K. M. Yoo, F. Liu, and R. R. Alfano, "Imaging objects hidden in scattering media using an absorption technique," Opt. Lett. **16**, 1068–1070 (1991).
12. E. Leith, H. Chen, Y. Chen, D. Dilworth, J. Lopez, R. Masri, J. Rudd, and J. Valdmanis, "Electronic holography and speckle methods for imaging through tissue using femtosecond gated pulses," Appl. Opt. **30**, 4204–4210 (1991).
13. M. R. Hee, J. A. Izatt, J. M. Jackobson, J. G. Fujimoto, and E. A. Swanson, "Femtosecond transillumination optical coherence tomography," Opt. Lett. **18**, 950–952 (1993).

14. V. V. Lyubimov, "Image transfer in a plane layer of a scattering medium and estimation of the resolving power of optical tomography using 1st transmitted photons of ultrashort pulses," Opt. Spectrosc. **76**, 725–726 (1994).
15. V. V. Lyubimov, "Spatial resolution in probing a strongly scattering medium with a short optical pulse," Opt. Spectrosc. **78**, 259–260 (1995).
16. E. N. Leith, B. G. Hoover, D. S. Dilworth, and P. P. Naulleau, "Ensemble-averaged Shack-Hartmann wavefront sensing for imaging through turbid media," Appl. Opt. **37**, 3643–3650 (1998).
17. V. V. Lyubimov, "On the spatial resolution of optical tomography of strongly scattering media with the use of the directly passing photons," Opt. Spectrosc. **86**, 251–252 (1999).
18. J. R. Singer, F. A. Grunbaum, P. Kohn, and J. P. Zubelli, "Image reconstruction of the interior of bodies that diffuse radiation," Science **248**, 990–993 (1990).
19. S. R. Arridge, P. van der Zee, M. Cope, and D. T. Delpy, "New results for the development of infrared absorption imaging," in *Biomedical Image Processing*, A. C. Bovik and W. E. Higgins, eds., Proc. SPIE **1245**, 92–103 (1991).
20. R. L. Barbour, H. L. Graber, R. Aronson, and J. Lubowsky, "Imaging of subsurface regions of random media by remote sensing," in *Time-Resolved Spectroscopy and Imaging of Tissues*, B. Chance, ed., Proc. SPIE **1431**, 192–203 (1991).
21. J. Schotland and J. S. Leigh, "Photon diffusion imaging," Biophys. J. **61**, 446 (1992).
22. C. P. Gonatas, M. Ishii, J. S. Leigh, and J. C. Schotland, "Optical diffusion imaging using a direct inversion method," Phys. Rev. E **52**, 4361–4365 (1995).
23. M. Ishii, J. S. Leigh, and J. C. Schotland, "Photon diffusion imaging of model and biological systems," in *Optical Tomography, Photon Migration and Spectroscopy of Tissue and Model Media: Theory, Human Studies*, B. Chance, ed., Proc. SPIE **2389**, 312–317 (1995).
24. M. O'Leary, D. Boas, B. Chance, and A. G. Yodh, "Experimental images of heterogeneous turbid media by frequency-domain diffusing photon tomography," Opt. Lett. **20**, 426–429 (1995).
25. V. V. Lyubimov, "Optics of photon density waves in strongly scattering media and spatial resolution in tomography," Opt. Spectrosc. **81**, 299–301 (1996).
26. J. C. Schotland, "Continuous wave diffusion imaging," J. Opt. Soc. Am. A **14**, 275–279 (1997).
27. V. B. Volkonskii, O. V. Kravtsenyuk, V. V. Lyubimov, E. P. Mironov, and A. G. Murzin, "The use of statistical characteristics of photon trajectories for the tomographic studies of optical macroheterogeneities in strongly scattering objects," Opt. Spectrosc. **86**, 253–260 (1999).
28. O. V. Kravtsenyuk and V. V. Lyubimov, "Specific features of statistical characteristics of photon trajectories in a strongly scattering medium near an object surface," Opt. Spectrosc. **88**, 608–614 (2000).
29. S. R. Arridge, "Optical tomography in medical imaging," Inverse Probl. **15**, R41–R93 (1999).
30. S. R. Arridge and W. R. B. Lionhart, "Nonuniqueness in diffusion-based optical tomography," Opt. Lett. **23**, 882–884 (1998).
31. C. L. Matson, "A diffraction tomographic model of the forward problem using diffuse photon density waves," Opt. Express **1**, 6–11 (1997), http://www.opticsexpress.org.
32. X. D. Li, T. Durduran, A. G. Yodh, B. Chance, and D. N. Pattanayak, "Diffraction tomography for biochemical imaging with diffuse-photon density waves," Opt. Lett. **22**, 573–575 (1997).
33. D. N. Pattanayak and A. G. Yodh, "Diffuse optical 3D-slice imaging of bounded turbid media using a new integro-differential equation," Opt. Express **4**, 231–240 (1999) http://www.opticsexpress.org.
34. X. Li, D. N. Pattanayak, T. Durduran, J. P. Culver, B. Chance, and A. G. Yodh, "Near-field diffraction tomography with diffuse photon-density waves," Phys. Rev. E **61**, 4295–4309 (2000).
35. The right-hand side of this equation is the same in different versions of perturbation theory, such as the first Born approximation or the first Rytov approximation, but the definition of the data function ϕ is different. Definition (10) is obtained in the first Born approximation; reexponentiation according to the Rytov expansion leads to $\phi(\mathbf{r}_1, \mathbf{r}_2) = -G_0(\mathbf{r}_1, \mathbf{r}_2)\ln[G(\mathbf{r}_1, \mathbf{r}_2)/G_0(\mathbf{r}_1, \mathbf{r}_2)]$.
36. B. Chu, E. Gulari, and E. Gulari, "Photon correlation measurements of colloidal size distributions. II. Details of histogram approach and comparison of methods of data analysis," Phys. Scr. **19**, 476–485 (1979).
37. I. Ersh, L. S. Muratov, S. Y. Novozhilov, B. M. Stockman, and M. I. Stockman, "Kinetics of the immunological reaction of agglutination and rapid determination of bacteria using an automated laser photon-correlation spectrometer," Dok. Biochem. **287**, 125–129 (1986).
38. R. Bauer, M. Hansen, S. Hansen, L. Ogendal, S. Lomholt, and K. Qvist, "The structure of casein aggregates during renneting studied by indirect Fourier transformation and inverse Laplace transformation of static and dynamic light scattering data, respectively," J. Chem. Phys. **103**, 2725–2737 (1995).
39. P. K. Venkatesh, R. W. Carr, M. H. Cohen, and A. M. Dean, "Microcanonical transition state theory rate coefficients from thermal rate constants via inverse Laplace transformation," J. Phys. Chem. A **102**, 8104–8115 (1998).
40. E. Schnedermann, "The inverse Laplace transform as the ultimate tool for transverse mass spectroscopy," Z. Phys. C **64**, 85–90 (1994).